# Anticancer Activity of Synthesized ZnO and ZnO/AgCl Nanocomposites against Five Human Cancer Cells

**Fattima Al-Zahra Gabar Gassim[1*] and Ali Jabbar Jasim Makkawi[2]**

[1]*Department of Pharmaceuticals, College of Pharmacy, University of Babylon, Hilla 51002, Iraq*

[2]*Department of Chemistry, College of Science, University of Babylon, Ministry of Education, Hilla 51002, Iraq*

* ***Corresponding author:***

*tel: +964-07725741416*
*email: alzahraafatema6@gmail.com*

*Received: August 5, 2022*
*Accepted: December 12, 2022*

**DOI:** 10.22146/ijc.76872

***Abstract:*** *In this work, a refluxing method is used to prepare nanoparticles of zinc oxide (ZnO NPS) and zinc oxide /silver chloride nanocomposites (ZnO/AgCl NCS). The structural properties of nanocrystals are studied by Atomic Force Microscope (AFM), X-Ray Diffraction (XRD), and Field Emission Scanning Electron Microscopy (FE-SEM) to determine the average crystal size, morphology, particle size and average grain size of nanocrystals. The results of anticancer efficiency of ZnO NPs and ZnO/AgCl NCs show cytotoxic activity against five human cancer cells, namely hepatocellular carcinoma, rhabdomyosarcoma (RD), colorectal carcinoma (HCT116), mammary gland (MCF-7), and epidermoid carcinoma (Hep2) compared against doxorubicin. The anticancer mechanism of pure and nanocomposites ZnO are suggested according to the release of $Zn^{+2}$ and the production of reactive oxidation species (ROS) and the effect of these species on cancer inhibition.*

***Keywords:*** *ZnO nanoparticles; the anticancer activity of nanoparticles; ZnO/AgCl nanocomposites*

## ■ INTRODUCTION

Doxorubicin is one of the most important anticancer (cytotoxic or antineoplastic) drugs used in high doses, but these drugs have had severe side effects. So, another drug with the same high activity and safety should be used. Nano-medicine techniques have paved the way for new targeted cancer therapies by allowing therapeutic compounds to be encapsulated in nanomaterials and selectively delivered to cancers by active uptake mechanisms and passive permeation. Resistance, to treatment, is one of the most important obstacles to conventional treatment [1]. Nanomedicine is the most important application of nanotechnology in medical problems because nanostructures of different shapes exhibit new and greatly enhanced physical, biological and chemical properties as well as distinct phenomena and functions [2-3]. Nano-systems were used to treat cancer by different nanotechnologies as shown in Fig. 1.

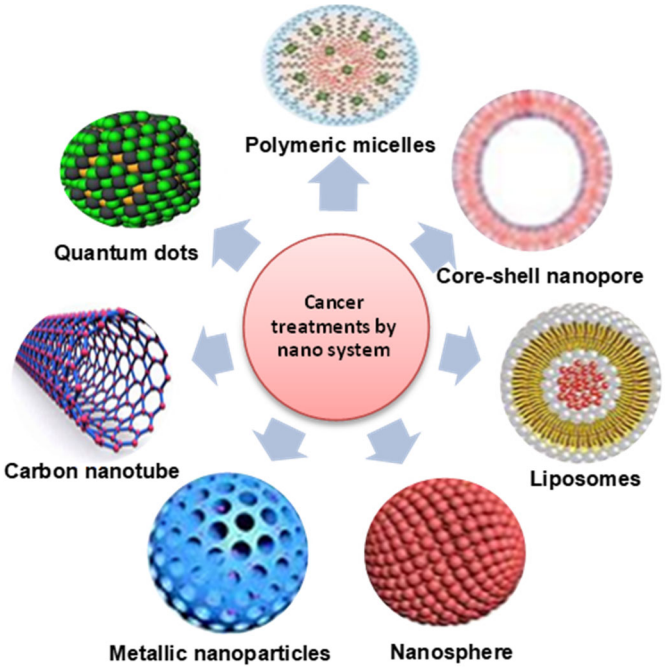


**Fig 1.** The schematic diagram represents various nanotechnologies that use nano-systems to treat cancer

Zinc oxide nanoparticles (ZnO NPs) have remarkable properties due to their ability the treatment of different kinds of cancers because of their biodegradability, biocompatibility [4], and unique physical and chemical features [5-6]. ZnO NPs have been exploited in preclinical and biomedical research, including drug delivery and cellular imaging [7-8]. ZnO absorbs UV rays at wavelengths ranging between 350–380 nm to produce reactive oxidation species (ROS) [9-10] so this semiconductor was modified by loading noble metals such as Ag on the surface of ZnO nanostructures to improve the image stability, it promotes efficiency in separating electron and hole pairs for photo-generation and expands light absorption of the visible region [11]. ROS plays an important role mechanism of ZnO NPs cytotoxicity through oxidative stress [12].

The aim of this study is to use pure and loaded ZnO NPs as anticancer materials as a new biomedical drug [4] instead of doxorubicin to decrease the dangerous side effect of this drug on the human body.

## ■ EXPERIMENTAL SECTION

### Materials

The materials used in this study were zinc acetate dihydrate ($Zn(CH_3COO)_2{\cdot}2H_2O$)) (99% purity, Sigma Aldrich (USA), silver nitrate ($AgNO_3$), zinc nitrate tetrahydrate ($Zn(NO_3)_2{\cdot}4H_2O$) (98% purity HANNOVER), and sodium chloride are produced from HANNOVER. While high-quality absolute ethanol and sodium hydroxide (99% purity Merck) is obtained from Germany.

### Instrumentation

The instrumentations used in this study were X-Ray Diffraction Spectroscopy (D5000 XRD6000, Shimadzu, Japan), Filed Emission Scanning Electron Microscopy (INSPECT S50 FEL (USA)), and Atomic Force Microscopy (Sartorius Arium 611).

### Procedure

#### *ZnO NPs preparation*

One pot refluxing method was used in the preparation of ZnO NPs. A 22 g of zinc acetate was dissolved in 600 mL of absolute ethanol. The solution was heated it to 60 °C for 30 min. The second solution was prepared by dissolving 25.2 g of oxalic acid in 400 mL of absolute ethanol then heated to 50 °C and then mixed with the above solution under constant stirring for 4 h. After that, the thick solution was dried at 80 °C overnight to produce a white powder of ZnO NPs [13].

#### *Modification of ZnO NPs*

Oleic acid was used as a coupling agent to modify the surface of nanoparticles to make the surface of ZnO NPs more hydrophobic dispersed in the organic area. This modification consists of dissolving 9 mL of oleic acid in 300 mL *o*-xylene to produce a solution of oleic acid. Then, recently 6 g of synthesized nanoparticles were added to the oleic acid solution. Then the reaction was allowed under stirring at 50 °C for 1 h. Then, nanoparticles were centrifuged for 15 min at 15000 rpm and washed with toluene, to remove un-reacted coupling agents. Finally, ZnO NPs were dried for one night at room temperature [14].

#### *ZnO/AgCl nanocomposites preparation*

ZnO/AgCl NCs were prepared by dissolving 2.110 g of $AgNO_3$ and 5.220 g of $Zn(NO_3)_2{\cdot}4H_2O$ in 50 mL of deionized water under constant stirring at room temperature. After that, an aqueous solution of NaOH (5 M) was added dropwise until the pH of the solution reached 10. After that, 1.450 g of NaCl was dissolved in 20 mL of deionized water. An aqueous solution of NaCl was added to the above solution. The suspension was refluxed for 3 h at about 90 °C. The solution was centrifuged to separate the grey precipitate. This precipitate was washed twice with deionized water and absolute ethanol. After that, the grey precipitate was dried at 600 °C overnight. Then ceramic slurry was used for crushing nanocomposites powder. The final nanocomposites were produced by calcination of the grey powder at 2000 °C for 1 h [15] (see Fig. 2). The reactions to obtain ZnO/AgCl NCs are written as follows:

$$Zn(NO_3)_2 \cdot 4H_2O + AgNO_3 + 3NaOH \rightarrow Zn(OH)_2 + AgOH + 3NaNO_3 + 4H_2O \quad (1)$$

$$AgOH + NaCl \rightarrow AgCl + NaOH \quad (2)$$

$$Zn(OH)_2 + AgCl \xrightarrow{\text{reflexing}} AgCl/ZnO + H_2O \quad (3)$$

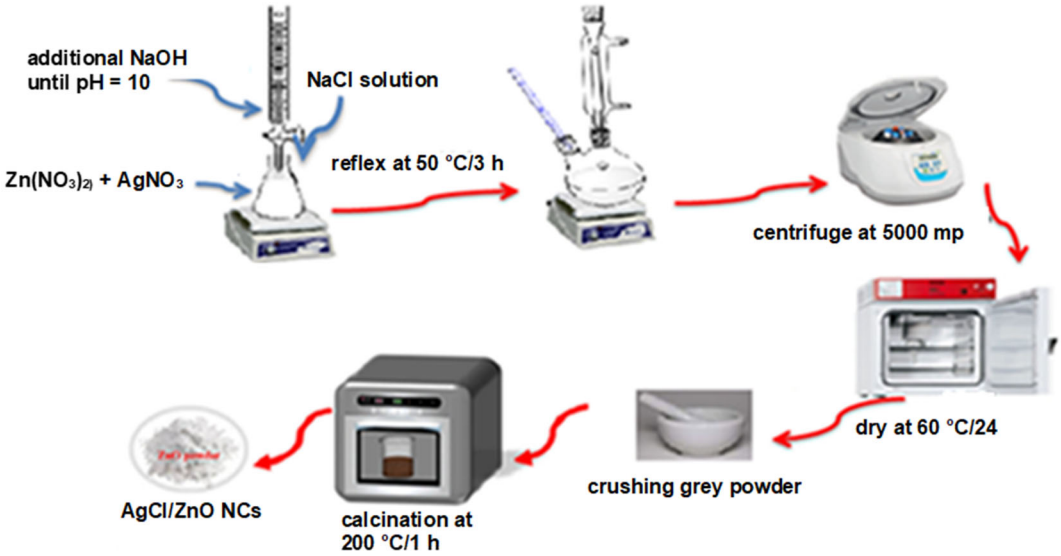


**Fig 2.** The schematic diagram for the steps for synthesizing AgCl/ZnO nanocomposites

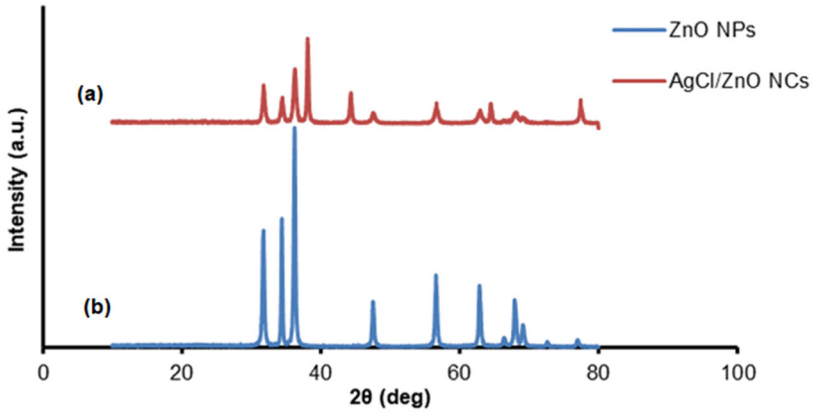


**Fig 3.** XRD patterns for ZnO NPs and AgCl/ZnO nanocomposites

### *Antioxidant assays by ABTS*

ABTS method was used to determine antioxidant efficiency. This method consisted of adding 2 mL of ABTS solution (60 µM) to 3 mL $MnO_2$ suspension (25 mg/mL), in a phosphate buffer solution of (pH 7, 0.1 M). The mixture solution was shaken and filtered. Then the absorbance of the ABTS radical solution was measured at 734 nm. After that, spectroscopic grade MeOH:phosphate buffer (1:1) was added to 50 µL of 2 µm solutions of the AgCl/ZnO NCs. The absorbance was adjusted, and the inhibition percentage was determined by the reduction in color intensity [16]. A blank sample consists of MeOH/phosphate buffer (1:1) instead of tested nanocomposites. ABTS inhibition of each sample was estimated by the following equation.

$$\text{ABTS}\ (\%\ \text{inhibition}) = \frac{\text{Abs}_{\text{control}} - \text{Abs}_{\text{test}}}{\text{Abs}_{\text{control}}} \times 100 \qquad (4)$$

## ■ RESULTS AND DISCUSSION

### XRD Analysis

Fig. 3(a) appears diffraction peaks of nacked ZnO at 2θ values 31.83°, 34.48°, 36.30°, 47.80°, 56.66°, 63.38°, and 68.48° which indicated hexagonal wurtzite structure of ZnO crystalline [17] (JCPDS 36-1451). Fig. 3(b) illustrated additional peaks at 2θ of 27.6°, 46.32°, 54.95°, 57.55°, 66.92°, 74.51°, and 76.71° indicating the presence of $Ag_2Cl$ NPs on the surface of ZnO nanoparticles [18]. Average size crystal (L) in nm were estimated by Scherrer's formula [19]

$$L = \frac{k\lambda}{\beta \cos\theta} \quad (5)$$

where k is the Scherrer's constant (0.94), λ is the wavelength of the X-ray radiation (0.15406 nm for Cukα), β is the full width of half-maximum (FWHM) intensity expressed in radians, and θ is a diffraction (Bragg) angle. The average crystallite sizes were estimated to be about 30.164 and 33.077 nm for pure ZnO NPs and ZnO/AgCl NCs, respectively.

## FE-SEM

FE-SEM was applied to observe the morphological properties and particle size of the prepared nanoparticles [20]. Fig. 4 shows FE-SEM images of the ZnO NPs and ZnO/AgCl NCs. The results of FE-SEM analysis show ZnO NPs have an individual sheets structure with particle size ranging between 18–41 nm. As shown in Fig. 4(a), SEM images of ZnO/AgCl NCs show a nanorod structure and the nanorods' diameter was ranged from 15–52 nm as appeared in Fig. 4(b).

## AFM

Fig. 5 and 6 illustrate the average diameters for both prepared samples are bigger than the values present for the size of the crystals indicating that each particle consists of several crystals (multi crystals) [21].

## Anticancer Activity

Cytotoxic efficiency of ZnO-NPs and ZnO/AgCl NCs was evaluated and compared against doxorubicin. The results of the cytotoxicity assessment of ZnO NPs and ZnO/AgCl NCs, against five human cancer cells Mammary gland (MCF-7), Hepatocellular carcinoma (HepG2), Colorectal carcinoma (HCT116),

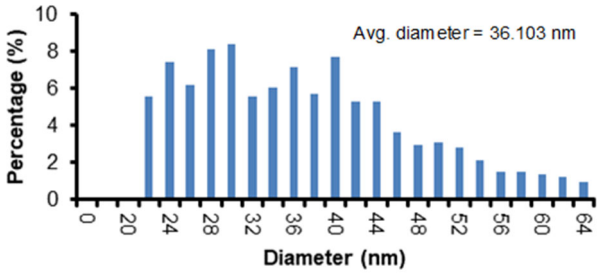


**Fig 5.** AFM cross-section analysis of ZnO NRs

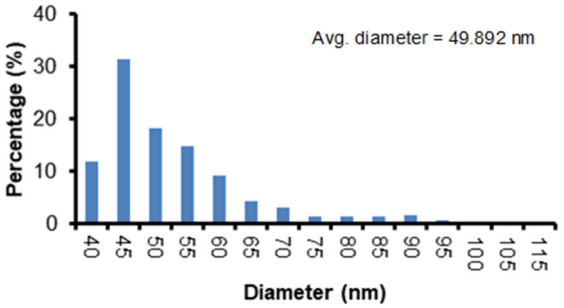


**Fig 6.** AFM cross-section analysis of ZnO/AgCl NCs

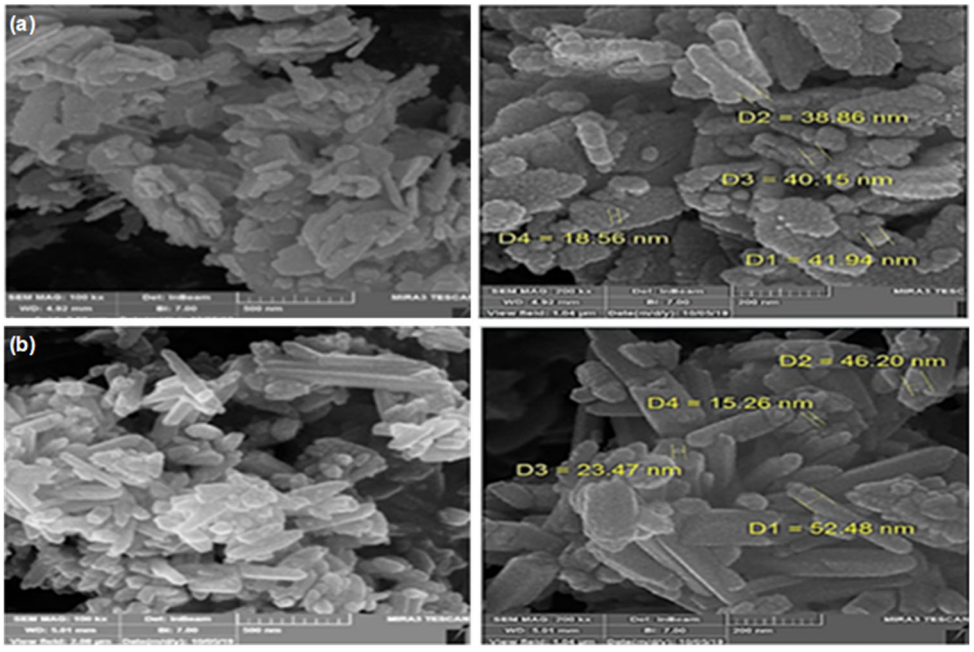


**Fig 4.** SEM images of (a) ZnO NPs and (b) ZnO-AgCl NCs nanocomposites

Epidermoid Carcinoma (Hep2), and Rhabdomyosarcoma (RD) are summarized in Table 1.

The results indicate that the *in vitro* cytotoxicity of $IC_{50}$ (μg) to all kinds of human cancer cells was moderate for pure ZnO NPs, while in the presence of ZnO/AgCl NCs the *in vitro* cytotoxicity of $IC_{50}$ (μg) to HCT116, Hep2, MCF-7, and HepG2 were strong, and RD was moderate. Fig. 7–9 explain the relative viability of cancer cells percentage (%) with various concentrations of doxorubicin, pure ZnO NPs, and ZnO/AgCl NCs. The results indicate that these percentages decreased with increasing of nanoparticles as a result of increasing interaction between prepared nanoparticles and cancer cells [22].

The mechanism of cytotoxicity from ZnO NPs and ZnO/AgCl NCs was based on the reactive oxidation species ROS ($O_2^{\bullet-}$, $OH^{\bullet}$, $H_2O_2$) generation through oxidative stress [23]. It is believed that intracellular oxidation species can connect the chain of mitochondrial electron transport, and it is suggested that

**Table 1.** *In vitro* $IC_{50}$ of ZnO NPs and ZnO/AgCl NCs against human tumor cells HepG2, HCT116, MCF-7, RD, and Hep2 compared to doxorubicin

| Compounds | *In vitro* cytotoxicity $IC_{50}$ (μg) | | | | |
|---|---|---|---|---|---|
| | HepG2 | HCT116 | MCF-7 | RD | Hep2 |
| DOX | 4.50 ± 0.2 | 5.23 ± 0.3 | 4.17 ± 0.2 | 6.10 ± 0.4 | 8.54 ± 0.6 |
| ZnO | 33.23 ± 3.2 | 37.09 ± 3.8 | 29.50 ± 2.7 | 47.08 ± 4.1 | 20.53 ± 2.3 |
| ZnO/AgCl# | 10.92 ± 1.3 | 11.15 ± 1.2 | 19.25 ± 1.9 | 24.93 ± 2.5 | 17.38 ± 1.4 |

$IC_{50}$ (μg): 1–10 (very strong), 11–20 (strong), 21–50 (moderate), 51–100 (weak) and above 100 (non-cytotoxic)

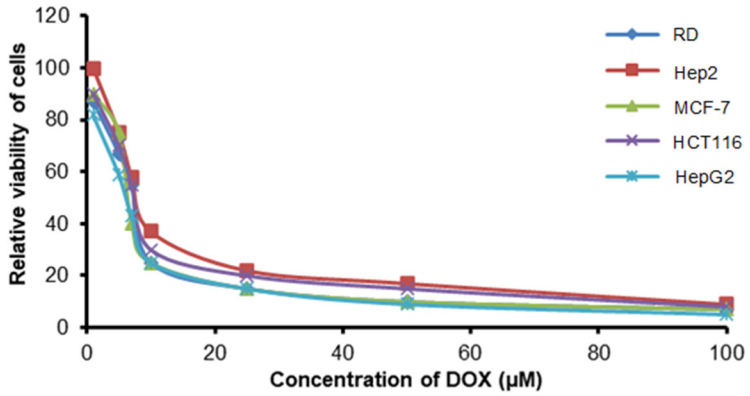


**Fig 7.** Relative viability of cells cancer (%) against the doxorubicin concentration (μM)

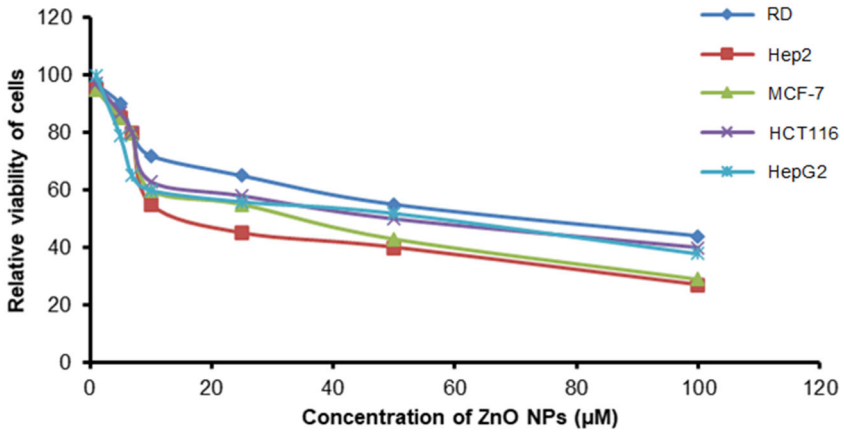


**Fig 8.** Relative viability of cells cancer (%) against the ZnO oxide nanoparticles concentration (μM)

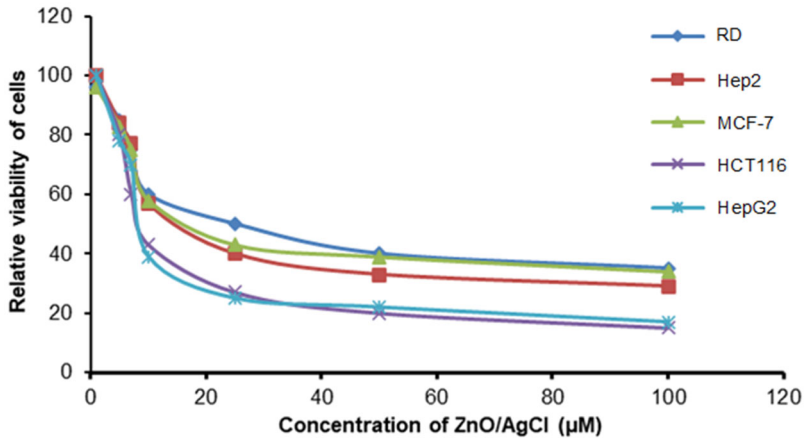


**Fig 9.** Relative viability of cells cancer (%) against the ZnO/AgCl nanocomposites concentration (μM)

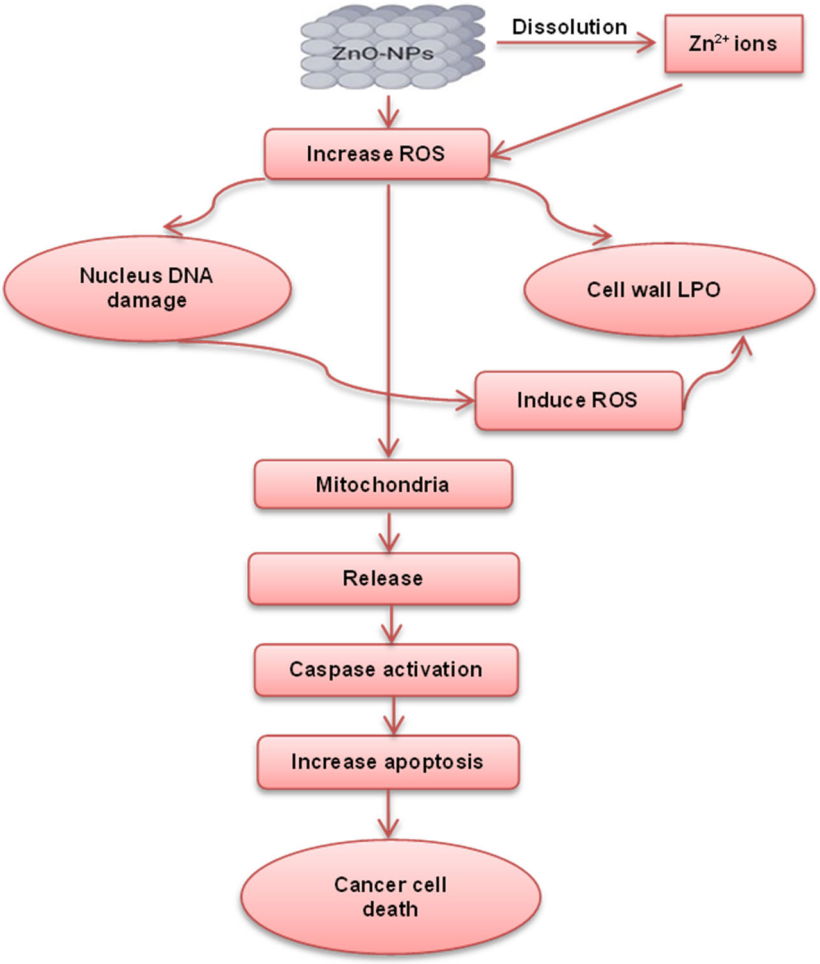


**Fig 10.** Schematic diagram of the possible mechanism for anticancer activity of ZnO NPs

the anticancer agents can attack cancer cells and damage the chain of electron transport due to the release of ROS intracellular [24]. Mitochondrial was damaged due to elevated levels of ROS then the balance of protein activities was lost, ultimately leading to apoptosis [25]. Dissolution of ZnO NPs causes increasing in intracellular levels of dissolved $Zn^{2+}$ and enhancing ROS production. These ROS disrupted the mitochondrial

membrane and caused the death of cancer cells via an apoptotic signaling pathway [26].

The results of Table 1 show increasing in anticancer activity by using ZnO/AgCl NCs as compared to pure ZnO NPs. This remark can be interpreted as the coupling of ZnO NPs with AgCl can reduce the band gap energy of ZnO (3.2 eV) and extend the excitation process from UV to the visible region [27]. Reducing the energy of band gap nanoparticles causes enhances the ability of these nanoparticles to generate oxidation species which leads to harm to the components of cancer cells [28]. A possible mechanism of ZnO NPs anticancer activity was illustrated in Fig. 10.

## ■ CONCLUSION

Pure ZnO NPs and ZnO/AgCl NCs were prepared. The structural properties of nanoparticles were investigated through XRD, FE-SEM, and AFM. Five human cancer cells (HCT116, HepG2, Hep-2, RD, and MCF-7) were used to examine anticancer activity for prepared samples. The previous studies were increasing anticancer potential by using ZnO/AgCl NCs as compared to pure ZnO NRs due to decreasing band gap energy of nanocomposites which lead to elevated levels of ROS and oxidative stress. Elevated ROS causes harm to the mitochondrial membrane and the destruction of cellular components such as DNA, lipids, proteins, and damage cells. The results show the anticancer activity of ZnO/AgCl NCs was increased as compared to naked ZnO NRs of cytotoxicity. The main mechanism of ZnO NPs and ZnO/AgCl NCs cytotoxicity results from ROS generation and release of $Zn^{2+}$ and $Ag^{1+}$ ions. Another mechanism suggested the formation of electrostatic forces on the surface of nanoparticles and the layered membrane of the cancer cell.

## ■ REFERENCES

[1] Ratan, Z.A., Haidere, M. F., Nurunnabi, M., Shahriar, S.M., Ahammad, A.J.S., Shim, Y.Y., Reaney, M.J.T., and Cho, J.Y., 2020, Green chemistry synthesis of silver nanoparticles and their potential anticancer effects, *Cancers*, 12 (4), 855.

[2] Abdolmaleki, A., Asadi, A., Gurushankar, K., Shayan, T.K., and Sarvestani, F.A., 2021, Importance of nano medicine and new drug therapies for cancer, *Adv. Pharm. Bull.*, 11 (3), 450–457.

[3] Hussain, A., Oves, M., Alajmi, M.F., Hussain, I., Amir, S., Ahmed, J., Rehman, M.T., El-Seedi, H.R., and Ali, I., 2019, Biogenesis of ZnO nanoparticles using *Pandanus odorifer* leaf extract: Anticancer and antimicrobial activities, *RSC Adv.*, 9 (27), 15357–15369.

[4] Anjum, S., Hashim, M., Malik, S.A., Khan, M., Lorenzo, J.M., Abbasi, B.H., and Hano, C., 2021, Recent advances in zinc oxide nanoparticles (ZnO NPs) for cancer diagnosis, target drug delivery, and treatment, *Cancers*, 13 (18), 4570.

[5] Wang, J., Gao, S., Wang, S., Xu, Z., and Wei, L., 2018, Zinc oxide nanoparticles induce toxicity in CAL 27 oral cancer cell lines by activating PINK1/Parkin-mediated mitophagy, *Int. J. Nanomed.*, 13, 3441.

[6] Makkawi, A.J.J., Aysa, N.H., and Gassim, F.A.G., 2019, Anticancer activity of zinc oxide and zinc oxide/cadmium sulfide nanocomposites, *Asian J. Pharm. Clin. Res.*, 12 (2), 535–539.

[7] Sawant, V.J., and Bamane, S.R., 2018, PEG-beta-cyclodextrin functionalized zinc oxide nanoparticles show cell imaging with high drug payload and sustained pH responsive delivery of curcumin in to MCF-7 cells, *J. Drug Delivery Sci. Technol.*, 43, 397–408.

[8] Safdar Ali, R., Meng, H., and Li, Z., 2022, Zinc-based metal-organic frameworks in drug delivery, cell imaging, and sensing, *Molecules*, 27 (1), 100.

[9] Xiong, H.M., 2013, ZnO nanoparticles are applied to bioimaging and drug delivery, *Adv. Mater.*, 25 (37), 5329–5335.

[10] Hashimoto, H., Tanino, R., Nakamura, M., and Fujita, Y., 2015, Surface treatment of zinc oxide nanoparticles by silica coating and evaluation of their dispersibility and photoluminescent properties, *e-J. Surf. Sci. Nanotechnol.*, 13, 451–454.

[11] Khatami, M., Varma, R.S., Zafarnia, N., Yaghoobi, H., Sarani, M., and Kumar, V.G., 2018, Applications of green synthesized Ag, ZnO and Ag/ZnO nanoparticles for making clinical antimicrobial wound-healing bandages, *Sustainable Chem. Pharm.*, 10, 9–15.

[12] Ng, C.T., Yong, L.Q., Hande, M.P., Ong, C.N., Yu, L.E., Bay, B.H., and Baeg, G.H., 2017, Zinc oxide nanoparticles exhibit cytotoxicity and genotoxicity through oxidative stress responses in human lung fibroblasts and *Drosophila melanogaster*, *Int. J. Nanomed.*, 12, 1621–1637.

[13] Chica, A., Gatti, G., Moden, B., Marchese, L., and Iglesia, E., 2006, Selective catalytic oxidation of organosulfur compounds with *tert*-butyl hydroperoxide, *Chem. - Eur. J.*, 12 (7), 1960–1967.

[14] Aysa, N.H., Al-Maamori, M.H., and Al-Maamori, N.A.A., 2017, Preparation and surface modification of zinc oxide nanoparticles, *J. Univ. Babylon Pure Appl. Sci.*, 25 (2), 497–503.

[15] Pirhashemi, M., and Habibi-Yangjeh, A., 2014, Preparation of AgCl–ZnO nanocomposites as highly efficient visible-light photocatalysts in water by a one-pot refluxing method, *J. Alloys Compd.*, 601, 1–8.

[16] Xiao, F., Xu, T., Lu, B., and Liu, R., 2020, Guidelines for antioxidant assays for food components, *Food Front.*, 1 (1), 60–69.

[17] Kavitha, R., 2018, Antidiabetic and enzymatic antioxidant potential from ethanolic extracts of leaf and fruit of *Trichosanthes dioica* and leaf of *Clitoria ternatea* on diabetic rats induced by streptozotocin, *Asian J. Pharm. Clin. Res.*, 11 (5), 233–239.

[18] Bazant, P., Kuritka, I., Munster, L., and Kalina, L., 2015, Microwave solvothermal decoration of the cellulose surface by nanostructured hybrid Ag/ZnO particles: A joint XPS, XRD and SEM study, *Cellulose*, 22 (2), 1275–1293.

[19] Ai, L., Zhang, C., and Jiang, J., 2013, Hierarchical porous AgCl@Ag hollow architectures: Self-templating synthesis and highly enhanced visible light photocatalytic activity, *Appl. Catal., B*, 142-143, 744–751.

[20] Gabar Gassim, F.A.Z., Makkaw, A.J., and Aysa, N.H., 2021, Removal of mercury(II) in aqueous solution by using ZnO and ZnO/CdS nanoparticles as photocatalysts, *Iran. J. Catal.*, 11 (4), 397–403.

[21] Savaloni, H., and Savari, R., 2018, Nano-structural variations of ZnO:N thin films as a function of deposition angle and annealing conditions: XRD, AFM, FESEM and EDS analyses, *Mater. Chem. Phys.*, 214, 402–420.

[22] Weiss, C., McLoughlin, P., and Cathcart, H., 2015, Characterisation of dry powder inhaler formulations using atomic force microscopy, *Int. J. Pharm.*, 494 (1), 393–407.

[23] Fan, M., Han, Y., Gao, S., Yan, H., Cao, L., Li, Z., Liang, X.J., and Zhang, J., 2020, Ultrasmall gold nanoparticles in cancer diagnosis and therapy, *Theranostics*, 10 (11), 4944–4957.

[24] Diebold, L., and Chandel, N.S., 2016, Mitochondrial ROS regulation of proliferating cells, *Free Radical Biol. Med.*, 100, 86–93.

[25] Moghimipour, E., Rezaei, M., Ramezani, Z., Kouchak, M., Amini, M., Angali, K.A., Dorkoosh, F.A., and Handali, S., 2018, Transferrin targeted liposomal 5-fluorouracil induced apoptosis *via* mitochondria signaling pathway in cancer cells, *Life Sci.*, 194, 104–110.

[26] Guo, C., Sun, L., Chen, X., and Zhang, D., 2013, Oxidative stress, mitochondrial damage, and neurodegenerative diseases, *Neural Regener. Res.*, 8 (21), 2003–2014.

[27] Jiang, J., Pi, J., and Cai, J., 2018, The advancing of zinc oxide nanoparticles for biomedical applications, *Bioinorg. Chem. Appl.*, 2018, 1062562.

[28] Pimpliskar, P.V., Motekar, S.C., Umarji, G.G., Lee, W., and Arbuj, S.S., 2019, Synthesis of silver-loaded ZnO nanorods and their enhanced photocatalytic activity and photoconductivity study, *Photochem. Photobiol. Sci.*, 18 (6), 1503–1511.